

PP1-Mediated Moesin Dephosphorylation Couples Polar Relaxation to Mitotic Exit

Patricia Kunda,^{1,4} Nelio T.L. Rodrigues,^{1,4}
Emadaldin Moeendarbary,² Tao Liu,¹ Aleksandar Ivetic,³
Guillaume Charras,² and Buzz Baum^{1,*}

¹MRC-Laboratory for Molecular Cell Biology,
University College London, London WC1E 6BT, UK

²London Centre for Nanotechnology, University College
London, London WC1H 0AH, UK

³James Black Centre, King's College London,
125 Coldharbour Lane, London SE5 9NU, UK

Summary

Animal cells undergo dramatic actin-dependent changes in shape as they progress through mitosis; they round up upon mitotic entry and elongate during chromosome segregation before dividing into two [1–3]. Moesin, the sole *Drosophila* ERM-family protein [4], plays a critical role in this process, through the construction of a stiff, rounded metaphase cortex [5–7]. At mitotic exit, this rigid cortex must be dismantled to allow for anaphase elongation and cytokinesis through the loss of the active pool of phospho-Thr559-moesin from cell poles. Here, in an RNA interference (RNAi) screen for phosphatases involved in the temporal and spatial control of moesin, we identify PP1-87B RNAi as having elevated p-moesin levels and reduced cortical compliance. In mitosis, RNAi-induced depletion of PP1-87B or depletion of a conserved noncatalytic PP1 phosphatase subunit Sds22 leads to defects in p-moesin clearance from cell poles at anaphase, a delay in anaphase elongation, together with defects in bipolar anaphase relaxation and cytokinesis. Importantly, similar cortical defects are seen at anaphase following the expression of a constitutively active, phosphomimetic version of moesin. These data reveal a new role for the PP1-87B/Sds22 phosphatase, an important regulator of the metaphase-anaphase transition, in coupling moesin-dependent cell shape changes to mitotic exit.

Results and Discussion

In *Drosophila* cells in culture, the Slik kinase has been shown to activate the actin-binding protein moesin through phosphorylation on Thr559, altering mitotic mechanics to drive mitotic cell rounding [2, 4]. It is not currently understood, however, how moesin dephosphorylation is regulated to enable the cortical relaxation required for anaphase elongation at mitotic exit. To explore this question, we carried out an RNA interference (RNAi) screen in the search for phosphatases necessary for efficient moesin dephosphorylation [8, 9]. The screen targeted 83 predicted phosphatases (see Table S1 available online) in *Drosophila* Kc167 (Kc) cells and identified a single serine/threonine phosphatase, PP1-87B, which when silenced led to a robust and dramatic increase in the levels of p-moesin

(Table S1). This was of interest because PP1 phosphatases have previously been implicated in the regulation of mitotic exit in *Drosophila* cells in culture [10], in mammalian cells, and in yeast [8, 10–14]. This role for PP1-87B in moesin dephosphorylation was confirmed by both immunofluorescence and western blotting using nonoverlapping double-stranded RNAs (dsRNAs) (Figures 1A and 1B; Figures S1A–S1C) and in a parallel study in S2 cells [7]. By combining PP1-87B and Slik dsRNAs, this elevated p-moesin signal was found to depend on the Slik kinase (Figures S1A and S1C). These data identify PP1-87B as the major regulator of moesin dephosphorylation in *Drosophila* cells in culture. Because ectopic moesin activation is sufficient to increase cortical rigidity in interphase cells [2], we tested whether PP1-87B RNAi is also able to mimic the effects of moesin activation on cell mechanics (Figure 1C). Using atomic force microscopy (AFM), we found that interphase cells depleted for PP1-87B exhibit a significant 2-fold increase in stiffness relative to control cells, as expected following an increase in phospho-moesin levels [2, 15].

Our next goal was to establish whether PP1-87B contributes to the regulation of the dynamic changes in moesin phosphorylation and localization during passage through mitosis [1, 2, 7]. Moesin is activated by phosphorylation as cells enter mitosis and has a uniform and isotropic cortical distribution in metaphase. P-moesin is then cleared from the cell poles at the onset of anaphase (Figure 2A) [1, 2], whereas a substantial proportion of the pool of total moesin remains at cell poles (Figure 2A; see Figure S2 for the equivalent in vivo data). When we used confocal microscopy to examine the effects of PP1-87B on the pool of p-moesin in individual mitotic Kc cells, we observed an overall increase in metaphase p-moesin levels (Figures S1B and S1C) together with a striking defect in clearance of p-moesin from cell poles at mitotic exit (Figures 2A and 2B). These data imply a role for PP1-87B in the regulation of cortical relaxation at the onset of anaphase. In order to determine whether this change in moesin regulation translates into a change in the shape of adherent cells as they pass through mitosis, we studied its function in S2R+ cells, which actively round up as they enter mitosis and flatten upon mitotic exit (Figure 2C; Figure S1D; [2]). The depletion of PP1-87B in S2R+ cells was found to induce a dramatic increase in the number of metaphase cells that appeared small and spherical in shape (from 40% in the lacZ RNAi cells to 90% in PP1-87B RNAi cells)—an effect that was accompanied by a significant 2-fold decrease in median metaphase cell length (Figure 2C; Figures S1D and S1E). Because spindle poles typically reach the cell edge, this may explain why it is that PP1-87B RNAi leads to a reduction in spindle length [16]. Furthermore, as seen in Kc cells, RNAi-induced depletion of PP1-87B in S2R+ cells inhibits anaphase elongation and the concomitant loss of actin filaments from cell poles (Figures 2C and 2D). Finally, we confirmed that the strong mitotic PP1-87B RNAi cell shape phenotype was rescued by the addition of Slik RNAi (Figures S1D and S1E). These data show that PP1-87B plays a specific role in the dynamic control of moesin-dependent cortical rigidity and mitotic cell shape.

⁴These authors contributed equally to this work

*Correspondence: b.baum@ucl.ac.uk

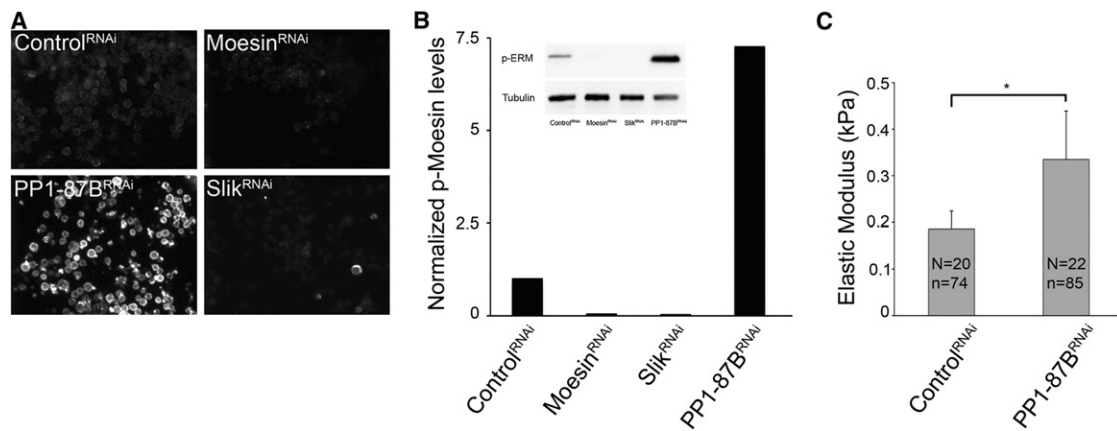


Figure 1. A Cell-Based RNAi Screen Identifies PP1-87B as a Key Regulator of Moesin Dephosphorylation

(A) PP1-87B was identified in a cell-based RNAi screen as a key regulator of pT599-moesin dephosphorylation in Kc167 cells. A representative image of p-moesin staining in wells of RNAi screen plates is shown for control (top left), moesin (top right), PP1-87B (bottom left), and Slik (bottom right) RNAi. (B) A western blot analysis in Kc167 cells confirms the increase in p-moesin levels following PP1-87B RNAi. The blot and quantification are representative of three independent experiments. Levels of protein were quantified using mean gray values in ImageJ using α -tubulin as a loading control. (C) PP1-87B depletion leads to an increase in cortical stiffness in S2R+ cells. Elastic moduli are shown for control and PP1-87B RNAi cells measured with atomic force microscopy. Error bars indicate the standard deviation and asterisks indicate significant differences between lacZ and PP1-87B RNAi cells. n indicates the total number of measurements and N indicates the number of cells.

PP1 catalytic subunits typically function in the context of a holoenzyme complex with one or more noncatalytic targeting subunits [8]. Therefore, it is expected that the functions of PP1 associated with mitotic exit [10, 17] involve one or more noncatalytic subunits. Although there is significant redundancy in the function and regulation of different PP1 complexes in many systems, PP1 has been shown to act together with a conserved noncatalytic subunit, Sds22, in the control of events at the metaphase-anaphase transition in both yeast and animal cells [12–14]. Furthermore, the conserved PP1 regulatory subunit Sds22 helps to limit p-moesin levels in *Drosophila* epithelia [18, 19] and has been reported to play a role along with PP1 in a *Drosophila* model of tumorigenesis and metastasis [20]. Therefore, having identified PP1-87B as a hit, we were keen to test the roles of Sds22 as part of our secondary analysis. In Kc cells, Sds22 RNAi induced a modest but variable increase in p-moesin levels (see Table S1). In addition, in contrast to Mbs, another noncatalytic PP1 subunit [21] and the other PP1 catalytic subunits (Figures S1D and S1E), Sds22 RNAi mimicked PP1-87B RNAi in accentuating the smooth, rounded form of the metaphase cortex of S2R+ cells (Figure S1D). Based on these observations, for the remainder of this study we chose to examine the functions of PP1-87B and Sds22 in parallel.

Active ERM proteins have been implicated in the regulation of mitotic cell shape in a stratified mammalian epithelium [22]. This prompted us to test the physiological roles of *Drosophila* PP1-87B and Sds22 within a tissue context. To do so, we chose the fly pupal notum as a model system, where the timing and path of epithelial cell divisions can be easily studied using a combination of loss-of-function genetics and live-cell imaging [23]. First, we confirmed that mitotic progression in this tissue is accompanied by dynamic changes in cell shape and parallel changes in the distribution of p-moesin (Figure 3). Entry into mitosis is accompanied by a progressive accumulation of p-moesin across the cortex as the cell rounds (Figures 3A and 3B). As cells begin to elongate at the onset of anaphase, p-moesin is then lost from cell poles and concentrated at the cell equator (Figure 3A). We calculated the ratio

of p-moesin levels at cell poles and the equator as a measure of the extent of this anaphase polarization. This was reproducibly <0.5 (Figures 3A and 3C). Importantly, this redistribution of p-moesin was accompanied by a comparatively modest shift in the localization of total moesin at early anaphase (Figure S2), leading to a polar/equatorial ratio for moesin of >0.8 (measured using an anti-moesin antibody [Figures S2C and S2D] and using moesin-GFP in live cells [Figures S2A and S2B] and in fixed tissue stained for both moesin-GFP and p-moesin [Figures S2E and S2F]). Similarly, we only observed a modest shift in the distribution of phosphomimetic T599D-moesin-GFP at anaphase (Figure 4A). Thus, p-moesin only makes up a proportion of the total pool of cortically localized moesin, and the subtle change in the distribution of total moesin (which Roubinet et al. [7] show is correlated with changes in the distribution of PIP2) cannot fully account for the significant shift in p-moesin localization seen upon entry into anaphase.

Having established the pattern of p-moesin dynamics in epithelial cells in wild-type nota, we used anti-pT599-moesin antibodies to survey levels of the active protein in animals expressing PP1-87B, Sds22, or Slik dsRNA (Figure 3A; Figure S2H). This confirmed an important role for Slik in moesin phosphorylation in this tissue (Figure S2H). By contrast, PP1-87B or Sds22 RNAi led to a dramatic increase in mitotic levels of p-moesin (Figures 3A and 3B). Most significantly, cells lacking PP1 phosphatase activity were unable to clear p-moesin from their poles following mitotic exit (Figures 3A–3C). This was not the result of a delay in the onset of anaphase, because a severe mitotic delay induced by RNAi-induced depletion of the APC4 subunit of the anaphase promoting complex had no measurable effect on the levels or distribution of p-moesin in metaphase or anaphase (Figures 3A–3C). Because moesin phosphorylation depends upon Slik, one might expect the effects of PP1-87B/Sds22RNAi to be reproduced in flies expressing high levels of the kinase. Strikingly, however, whereas increasing Slik expression (verified with antibody staining in Figure S2G) led to elevated levels of p-moesin in prophase and metaphase cells, similar to those seen in

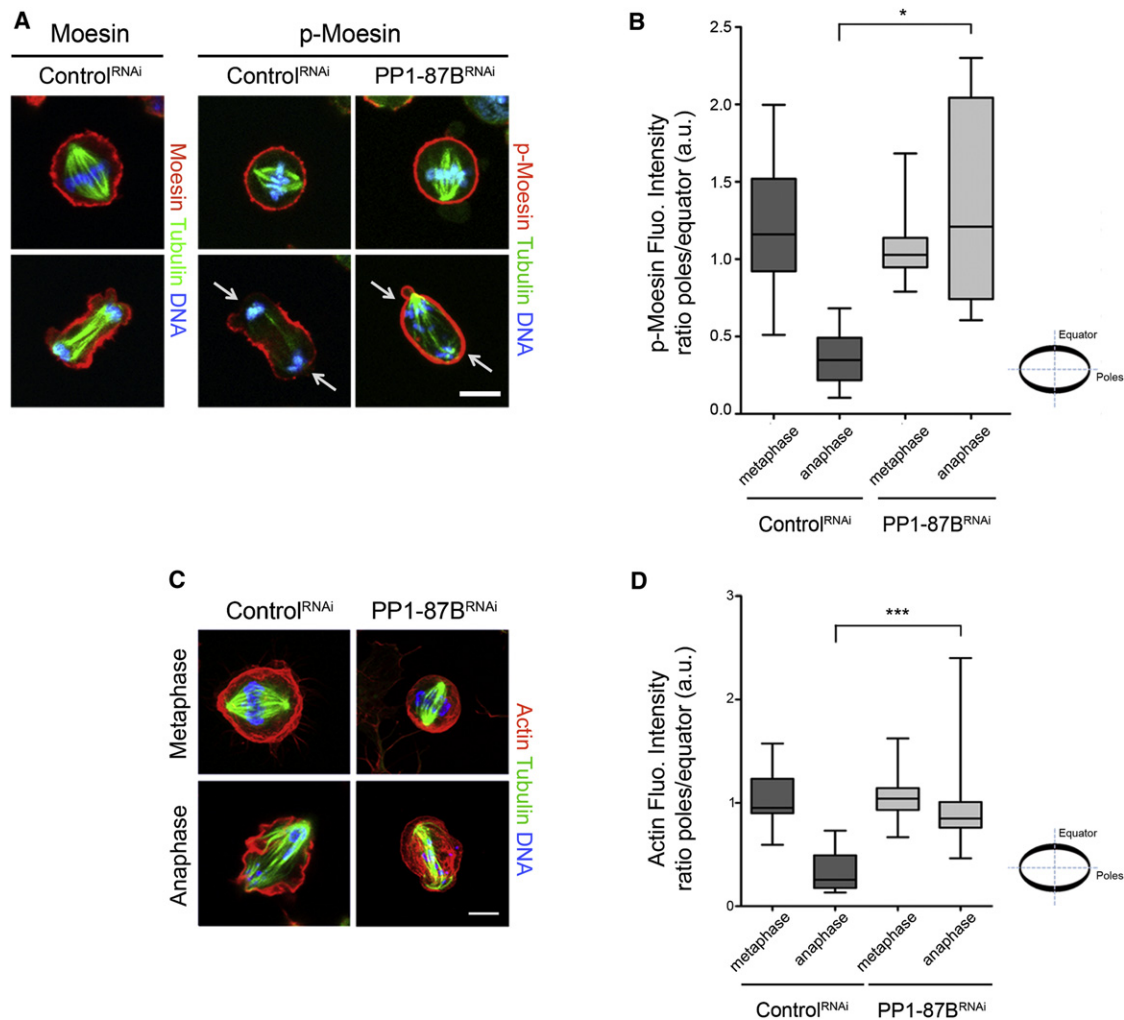


Figure 2. The PP1-87B Phosphatase Regulates the Levels and Localization of Moesin Phosphorylation during Mitotic Progression

(A) Confocal images showing the distribution of moesin (left) and p-moesin (right) in metaphase and anaphase Kc167 cells exposed to lacZ or PP1-87B dsRNA. PP1-87B depletion increases mitotic levels of p-moesin. A pool of total moesin remains at cell poles at anaphase (left panel). By contrast, p-moesin (right panel) has a uniform metaphase cortical localization but is cleared from the cell poles at anaphase in control cells through a process that requires PP1-87B (arrows). Images show single confocal sections. Scale bar represents 5 μ m.

(B) Differences between p-moesin levels at cell poles and the equator were calculated using a ratio of the mean gray value in ImageJ for ~ 10 randomly chosen cells and data were plotted as box and whisker plots. A nonparametrical Mann-Whitney test was used to confirm significance ($p < 0.05$) between control and PP1-87B RNAi cells in anaphase.

(C) Confocal images show actin filaments (red) in control and PP1-87B RNAi S2R+ cells (scale bar represents 5 μ m). Images correspond to 3D projections of confocal stacks.

(D) Relative levels of F-actin at cell poles and the equator were calculated for randomly chosen control and PP1-87B RNAi cells in metaphase ($n = 25$) and anaphase ($n = 25$). Mean gray values were calculated in ImageJ and the data were plotted as box and whisker plots. A nonparametrical Mann-Whitney test was used to confirm significance ($p < 0.001$) between control and PP1-87B RNAi cells in anaphase.

PP1-87B RNAi and Sds22 RNAi experiments, Slik overexpression had no visible effect on the loss of p-moesin upon mitotic exit or on its clearance from cell poles (Figures 3A–3C). In addition, we noted that it was only through expressing ectopic Slik that we observed a reproducible increase in interphase p-moesin levels. Thus, the accumulation of p-moesin upon entry into mitosis depends largely on Slik, whereas levels of p-moesin in mitosis are determined by the balance of Slik and PP1-87B/Sds22 activities, and it is the phosphatase alone that determines the kinetics of p-moesin loss upon mitotic exit.

It was important to determine how these changes in p-moesin levels impinge on mitotic cell shape. Following either the silencing of PP1-87B or Sds22 we observed a reproducible

and significant delay in the rate of polar relaxation at anaphase (Figures 4A and 4B; Figure S3A). Moreover, although the onset of cortical relaxation was symmetric in control cells, the majority of cells with reduced levels of PP1-87B or Sds22 initiated cortical relaxation at a single site (Figures 4A, 4D, and 4E). We confirmed using APC4 RNAi that this was not due to a metaphase delay (data not shown). Instead, given the role of p-moesin in the generation of a rigid cortex [2], this phenotype likely reflects a failure in the timely clearance of p-moesin at anaphase, preventing the orderly release of pressure at both cell poles that is required for bipolar anaphase elongation [24]. To test this idea directly, we used a phosphomimetic constitutively active form of full-length moesin, T559D-moesin-GFP.

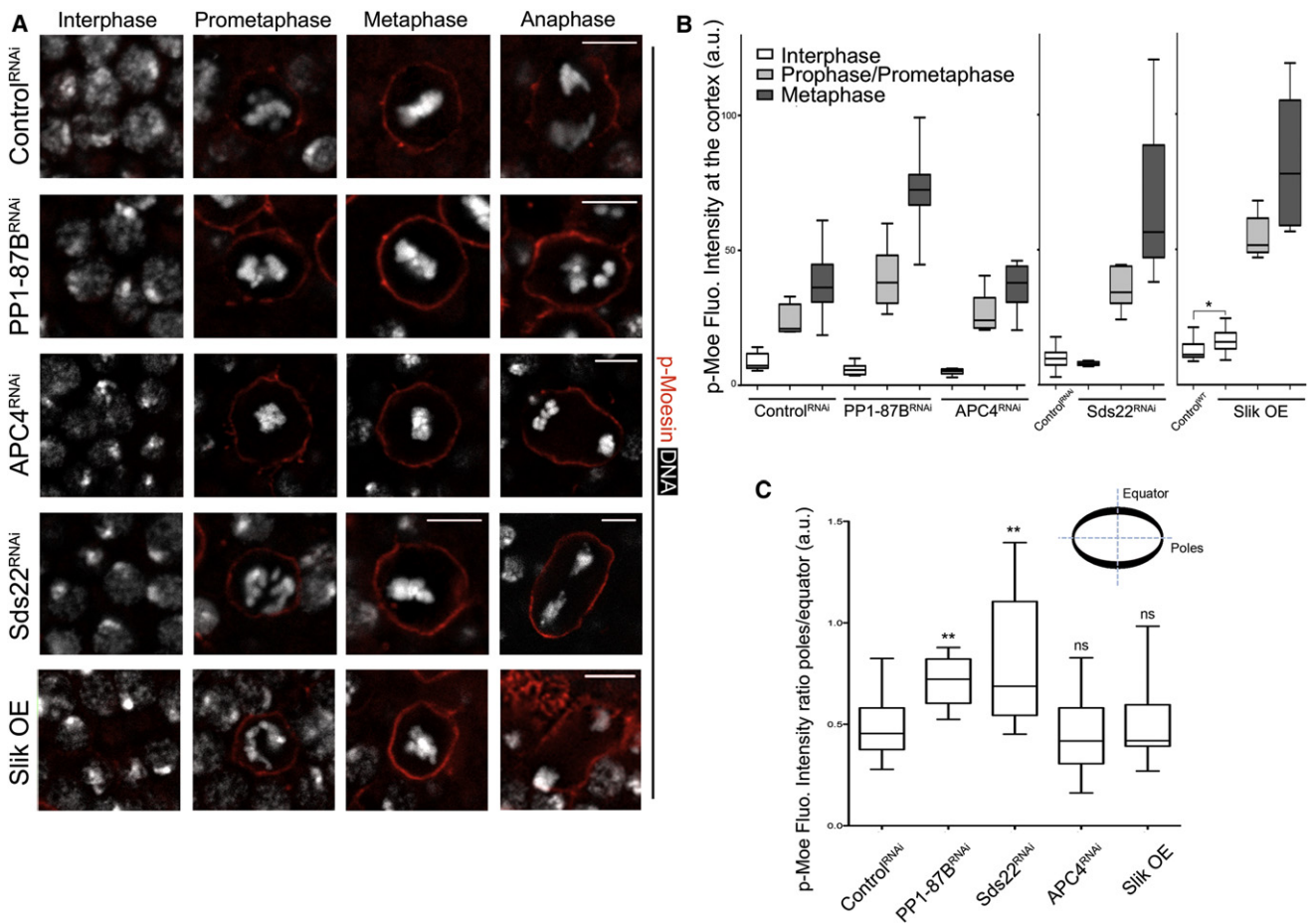


Figure 3. The Role of Slik and PP1-87B/ Sds22 in the Spatio-Temporal Regulation of p-Moesin Levels during Mitotic Progression in Developing *Drosophila* Pupae

(A) Panels show representative cells in interphase and at three different stages of mitosis in nota from control, PP1-87B RNAi, Sds22 RNAi, APC4 RNAi, and Slik overexpression (OE) animals. All samples were stained for p-moesin (red) to visualize its cortical levels at the different stages of mitosis. Mitotic progression was followed by DNA labeling (white) and MPM-2 or α -tubulin immunolabeling (data not shown). Tub::Gal80ts; Pnr::Gal4 flies were used as controls, whereas the remaining samples were prepared from flies expressing a UAS-inducible gene or gene-specific RNA hairpin. Five micrometer scale bars apply across rows of images.

(B) P-moesin levels at the cortex were quantified in multiple cells in the conditions featured in (A). Sds22 RNAi and Slik overexpression experiments were performed independently, although the experimental setup and imaging settings were identical. Data for both are presented along with control RNAi flies processed in parallel. For each mitotic stage, $n > 7$ cells from at least three animals in each background were measured. A nonparametrical Mann-Whitney test was used to confirm significance ($p < 0.05$) for the difference between control and Slik overexpressing cells in interphase.

(C) Graphs depict the ratio of p-moesin levels in anaphase cells at cell poles and the equator for each of the experiments. PP1-87B and Sds22 RNAi prevent polar clearance, when compared with control or APC4 RNAi cells or Slik overexpression. A nonparametrical Mann-Whitney test was used to confirm significance. Star signs indicate statistically significant differences between control and depletion conditions, and (ns) indicates data that were not significantly different ($p < 0.01$ for PP1-87B RNAi and Sds22 RNAi).

Strikingly, TD-moesin expression was sufficient to mimic the PP1-87B and Sds22 anaphase RNAi phenotype—leading to a significant reduction in the kinetics of anaphase elongation (Figures 4A and 4C; Figure S3B). In addition, in the majority of cases, TD-moesin expression induced the initiation of polar relaxation at a single cortical site (Figures 4A, 4D, and 4E), an event that was accompanied by the local loss of TD-moesin-GFP (Figures 4A, 4D, and 4E). These data provide strong support for the idea that PP1-87B/Sds22 acts via moesin dephosphorylation to induce a timely and orderly relaxation of the anaphase cell cortex [24]; even though Slik protein remains localized at cell poles (Figure S2G). Interestingly, failure to clear active moesin from the poles at anaphase led to severe defects in cell shape and blebbing during cytokinesis (Figure S4C). In addition, when we monitored the ability of

asymmetrically dividing PP1/Sds22 RNAi cells (P1 cells) to segregate cortically localized cell-fate determinants, we observed striking defects in their ability to form and position a normal Pon-GFP crescent at early stages of anaphase. These defects were partly but not completely resolved as cells completed cell division, when determinant segregation is known to become dependent on microtubule-based processes (Figure S4D) [25]. These results reinforce the notion that PP1-87B and Sds22 regulate cortical dynamics at mitotic exit.

To conclude, previous work in both animal cells [14] and in yeast [12, 13] has implicated PP1 in the regulation of mitotic exit, and in one case in the regulation of actin-dependent polar growth [26]. In agreement with this and as previously reported in *Drosophila*, we find that PP1-87B plays an important role in

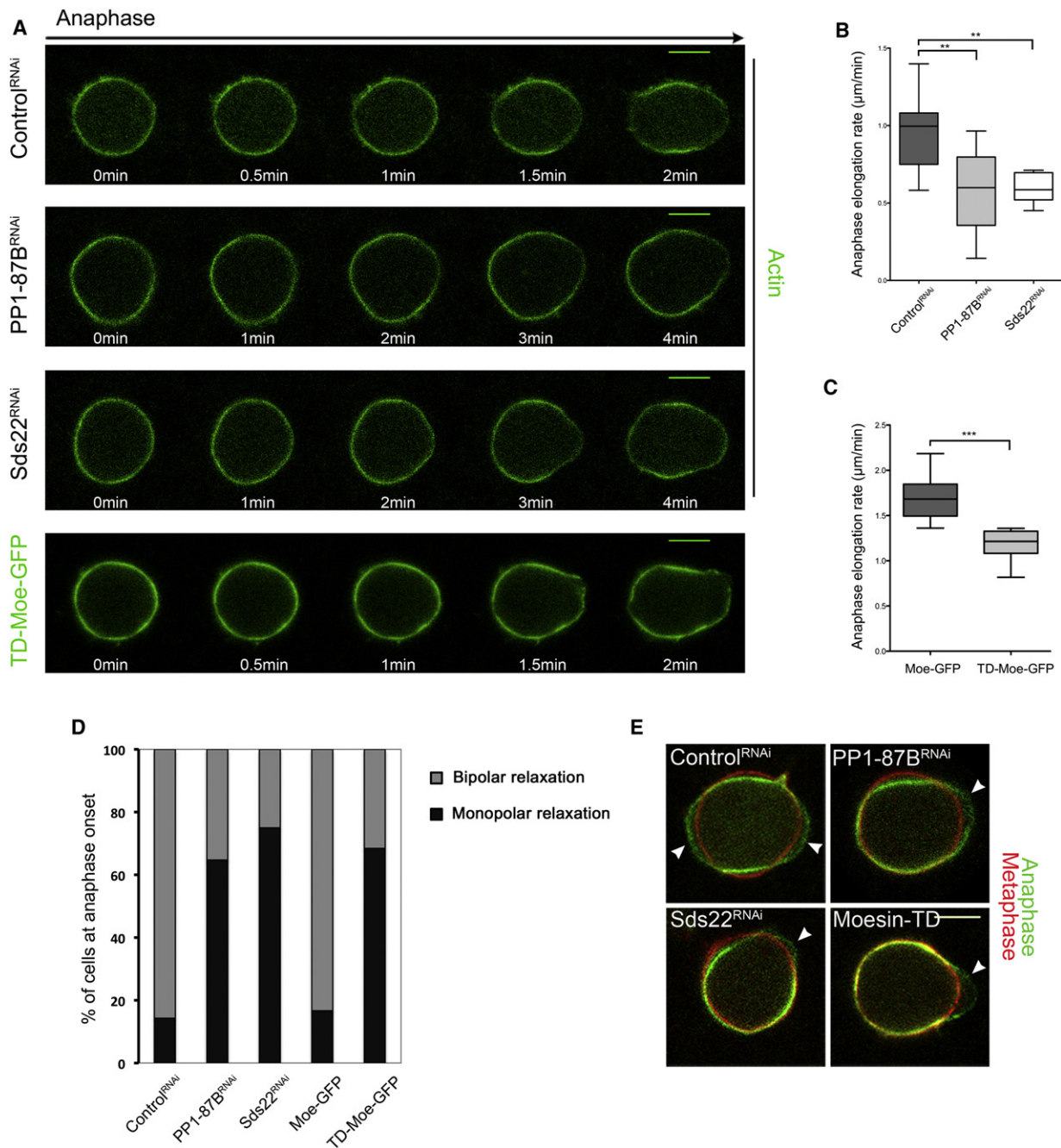


Figure 4. Depletion of PP1-87B or Sds22, or T559D-Moesin Overexpression All Compromise Timely, Bipolar Cell Relaxation at Anaphase

(A) The anaphase progression of individual P1 cells in control, PP1-87B RNAi, Sds22 RNAi, and T559D-moesin-GFP expressing backgrounds was visualized by confocal microscopy and is featured in four montages of representative cells. For the first three conditions, cells were marked with Neu::GMA to label actin filaments (data shown), and tubulin-RFP (data not shown) to follow the precise onset of anaphase. PP1-87B RNAi and Sds22 RNAi conditions perturb bipolar relaxation and decrease the rate of anaphase elongation. The overexpression of T559D-moesin-GFP, but not wild-type moesin-GFP (data not shown), mimics the defects in cortical relaxation observed in PP1-87B RNAi and Sds22 RNAi cells, where polar relaxation initiates at a single cortical site, which coincides with local loss of T559D-moesin-GFP.

(B) PP1-87B RNAi and Sds22 RNAi decrease the rate of anaphase elongation (as seen in A). Star signs indicate that the difference between control and each of the RNAi conditions is statistically significant ($p < 0.01$ for either RNAi condition; $n = 7$ cells from four control pupae; $n = 12$ from three PP1-87B RNAi pupae; $n = 8$ from four Sds22 RNAi pupae).

(C) Similarly, T559D-moesin-GFP expression delays anaphase progression relative to a wild-type moesin-GFP control ($p < 0.001$; $n = 8$ cells from four animals in each condition).

(D) The graph shows the proportion of cells in which anaphase initiates as a monopolar or bipolar relaxation in control, PP1-87B RNAi, Sds22 RNAi, moesin-GFP, and T559D-moesin-GFP expressing cells (control RNAi, $n = 8$; PP1-87B RNAi, $n = 17$; Sds22 RNAi, $n = 9$; moesin-GFP, $n = 6$; T559D-moesin-GFP, $n = 19$).

(E) False colored time-lapse images of representative cells show the superimposition of metaphase (red) and early anaphase (green) cortices. PP1-87B RNAi and Sds22 RNAi cells, and the majority of T559D-moesin-GFP expressing cells initiate relaxation at a single cortical site (see arrowheads). Time-lapse images in (A) and (E) show single confocal sections at the level of the mitotic spindle. Scale bars represent 5 μm. A nonparametrical Mann-Whitney test was used to confirm statistical significance.

the regulation of spindle morphogenesis and chromosome segregation at mitotic exit [10, 11, 16] (Figures S4A and S4B), which likely involves counteracting the effects of CENP-E phosphorylation by Aurora B to ensure the secure attachment of kinetochores to the mitotic spindle [17]. Here, we provide evidence to show that whereas Slik activity mediates the activation of moesin upon mitotic entry to stabilize the mitotic cortex in animal cells, PP1-87B/Sds22 specifically regulates the dephosphorylation of moesin at anaphase to induce polar relaxation. These findings suggest that PP1 performs a crucial and conserved function in coupling the dynamic regulation of cell shape to chromosome segregation in both fungi and animals. This coordination is likely to be critical for the accurate partitioning of DNA and cell contents at cell division.

Supplemental Information

Supplemental Information includes four figures, one table, and Supplemental Experimental Procedures and can be found with this article online at doi:10.1016/j.cub.2011.12.016.

Acknowledgments

We thank Cristian Acosta for his help with the statistical analyses, Barry Thompson, Nic Tapon, Rick Fehon, David Hipfner, Steve Cohen, François Payre, Dan Kiehart, the Vienna Drosophila RNAi Center, the NIG-Fly and the Bloomington Drosophila Stock Center for generously providing us with reagents and fly stocks. We also thank Jennifer Mummery-Widmer and Juergen Knoblich for sharing unpublished in vivo RNAi screen data. We are especially grateful to Cancer Research UK and the EU FP7 Cancer Pathways network for funding. G.C. was funded by the Royal Society, and E.M. was in receipt of a Dorothy Hodgkins Postgraduate Award from the Engineering and Physical Sciences Research Council. P.K. and N.R. were supported by Cancer Research UK, and B.B. was supported by the Royal Society, University College London, Wellcome, and Cancer Research UK.

Received: August 9, 2011

Revised: October 23, 2011

Accepted: December 6, 2011

Published online: December 29, 2011

References

- Carreno, S., Kouranti, I., Glusman, E.S., Fuller, M.T., Echard, A., and Payre, F. (2008). Moesin and its activating kinase Slik are required for cortical stability and microtubule organization in mitotic cells. *J. Cell Biol.* **180**, 739–746.
- Kunda, P., Pelling, A.E., Liu, T., and Baum, B. (2008). Moesin controls cortical rigidity, cell rounding, and spindle morphogenesis during mitosis. *Curr. Biol.* **18**, 91–101.
- Rosenblatt, J., Cramer, L.P., Baum, B., and McGee, K.M. (2004). Myosin II-dependent cortical movement is required for centrosome separation and positioning during mitotic spindle assembly. *Cell* **117**, 361–372.
- Fehon, R.G., McClatchey, A.I., and Bretscher, A. (2010). Organizing the cell cortex: the role of ERM proteins. *Nat. Rev. Mol. Cell Biol.* **11**, 276–287.
- Kunda, P., and Baum, B. (2009). The actin cytoskeleton in spindle assembly and positioning. *Trends Cell Biol.* **19**, 174–179.
- Roch, F., Polesello, C., Roubinet, C., Martin, M., Roy, C., Valenti, P., Carreno, S., Mangeat, P., and Payre, F. (2010). Differential roles of PtdIns(4,5)P2 and phosphorylation in moesin activation during Drosophila development. *J. Cell Sci.* **123**, 2058–2067.
- Roubinet, C., Decelle, B., Chicanne, G., Dorn, J.F., Payrastra, B., Payre, F., and Carreno, S. (2011). Molecular networks linked by Moesin drive remodeling of the cell cortex during mitosis. *J. Cell Biol.* **195**, 99–112.
- Barr, F.A., Elliott, P.R., and Gruneberg, U. (2011). Protein phosphatases and the regulation of mitosis. *J. Cell Sci.* **124**, 2323–2334.
- Liu, T., Sims, D., and Baum, B. (2009). Parallel RNAi screens across different cell lines identify generic and cell type-specific regulators of actin organization and cell morphology. *Genome Biol.* **10**, R26.
- Chen, F., Archambault, V., Kar, A., Lio, P., D'Avino, P.P., Sinka, R., Lilley, K., Laue, E.D., Deak, P., Capalbo, L., et al. (2007). Multiple protein phosphatases are required for mitosis in Drosophila. *Curr. Biol.* **17**, 293–303.
- Axton, J.M., Dombrádi, V., Cohen, P.T., and Glover, D.M. (1990). One of the protein phosphatase 1 isoenzymes in Drosophila is essential for mitosis. *Cell* **63**, 33–46.
- Ohkura, H., and Yanagida, M. (1991). *S. pombe* gene *sds22+* essential for a midmitotic transition encodes a leucine-rich repeat protein that positively modulates protein phosphatase-1. *Cell* **64**, 149–157.
- MacKelvie, S.H., Andrews, P.D., and Stark, M.J. (1995). The *Saccharomyces cerevisiae* gene *SDS22* encodes a potential regulator of the mitotic function of yeast type 1 protein phosphatase. *Mol. Cell Biol.* **15**, 3777–3785.
- Posch, M., Khoudoli, G.A., Swift, S., King, E.M., Deluca, J.G., and Swedlow, J.R. (2010). *Sds22* regulates aurora B activity and microtubule-kinetochore interactions at mitosis. *J. Cell Biol.* **191**, 61–74.
- Harris, A.R., and Charras, G.T. (2011). Experimental validation of atomic force microscopy-based cell elasticity measurements. *Nanotechnology* **22**, 345102.
- Goshima, G., Wollman, R., Stuurman, N., Scholey, J.M., and Vale, R.D. (2005). Length control of the metaphase spindle. *Curr. Biol.* **15**, 1979–1988.
- Kim, Y., Holland, A.J., Lan, W., and Cleveland, D.W. (2010). Aurora kinases and protein phosphatase 1 mediate chromosome congression through regulation of CENP-E. *Cell* **142**, 444–455.
- Ceulemans, H., Vulsteke, V., De Maeyer, M., Tatchell, K., Stalmans, W., and Bollen, M. (2002). Binding of the concave surface of the *Sds22* superhelix to the alpha 4/alpha 5/alpha 6-triangle of protein phosphatase-1. *J. Biol. Chem.* **277**, 47331–47337.
- Grusche, F.A., Hidalgo, C., Fletcher, G., Sung, H.H., Sahai, E., and Thompson, B.J. (2009). *Sds22*, a PP1 phosphatase regulatory subunit, regulates epithelial cell polarity and shape [*Sds22* in epithelial morphology]. *BMC Dev. Biol.* **9**, 14.
- Jiang, Y., Scott, K.L., Kwak, S.J., Chen, R., and Mardon, G. (2011). *Sds22*/PP1 links epithelial integrity and tumor suppression via regulation of myosin II and JNK signaling. *Oncogene* **30**, 3248–3260.
- Grassie, M.E., Moffat, L.D., Walsh, M.P., and MacDonald, J.A. (2011). The myosin phosphatase targeting protein (MYPT) family: a regulated mechanism for achieving substrate specificity of the catalytic subunit of protein phosphatase type 1δ. *Arch. Biochem. Biophys.* **510**, 147–159.
- Luxenburg, C., Pasolli, H.A., Williams, S.E., and Fuchs, E. (2011). Developmental roles for Srf, cortical cytoskeleton and cell shape in epidermal spindle orientation. *Nat. Cell Biol.* **13**, 203–214.
- Georgiou, M., Marinari, E., Burden, J., and Baum, B. (2008). Cdc42, Par6, and aPKC regulate Arp2/3-mediated endocytosis to control local adherens junction stability. *Curr. Biol.* **18**, 1631–1638.
- Sedzinski, J., Biro, M., Oswald, A., Tinevez, J.Y., Salbreux, G., and Paluch, E. (2011). Polar actomyosin contractility destabilizes the position of the cytokinetic furrow. *Nature* **476**, 462–466.
- Neumüller, R.A., and Knoblich, J.A. (2009). Dividing cellular asymmetry: asymmetric cell division and its implications for stem cells and cancer. *Genes Dev.* **23**, 2675–2699.
- Alvarez-Tabarés, I., Grallert, A., Ortiz, J.M., and Hagan, I.M. (2007). *Schizosaccharomyces pombe* protein phosphatase 1 in mitosis, endocytosis and a partnership with Wsh3/Tea4 to control polarised growth. *J. Cell Sci.* **120**, 3589–3601.